



Technical-economic Analysis of the Organic Rankine Cycle with Different Energy Sources

S. Amiri Hezaveh^a, S. D. Farahani^{b,*}, M. Alibeigi^c

^{a,b,c} *Department of Mechanical Engineering, Arak University of Technology, Arak, 38181-41167, Iran.*

Abstract

In this study, the thermodynamic and economical design of an organic Rankine cycle with different energy sources in Arak is investigated. R245fa, Isobutane, R114, R123, Isobutene and Toluene are considered as working fluid. The effects of organic fluids and pinch temperatures on the Rankine cycle performance were examined. The use of other energy sources such as solar energy, biomass, heat recovery from microturbine was Discussed and the cost of power generation was calculated. Isobutene has been selected as the operating fluid of the cycle for further investigation. According to the heat required by the Rankin cycle, the solar tower has been designed and estimated. The output power of the organic Rankine cycle using microturbine is increased by about 20%. The results show over 70% of the solar tower cost is related to mirrors. The highest cost of power generation is the use of microturbine, solar energy, biomass and hot water, respectively.

Keywords: Thermodynamic analyses; Thermal performance; hot water/solar system/micro turbine; fossil /Biomass

Introduction

The world is in need of energy. Because demand for non-renewable fuels is growing, and world consumption has reached a level it has never been before. Low temperature dissipative heat is usually released directly into the environment, which may not only cause thermal pollution but also cause environmental problems such as ozone depletion, global warming, and air pollution. Energy derived from fossil fuels is used in many Industry and power plants. With the increasing Worry on the environmental impact of fossil fuels, the utilization of

natural gas (NG) is growing, though coal and petroleum are still the elementary energy resources. Furthermore, NG has several property as an energy resource, including efficient ignition, easy forwarding and storage, and environmental friendliness [1]. However, there is concern about global warming due to the burning of fossil fuels and natural waste (biomass). Considering this, now, one can think of clean energy such as solar energy, which is a free and clean energy. One of the technologies that is able to recover heat dissipation in various industrial processes is called the organic Rankin cycle

(ORC). The simple organic Rankine cycle consists of four parts: condenser, pump, evaporator and turbine. The shape of the organic Rankine cycle considered for the thermodynamic design along with its entropy temperature diagram [2]. The scale of the systems is usually several hundred kilowatts, which in the ordinary steam cycles is changed to evaporators and other components of the cycle with The Rankine cycle is similar. The dissipated heat or low temperature in the evaporator is used to evaporate organic fluids. This high pressure steam expands through the turbine and generates power. The low pressure steam at the turbine outlet is distilled into the condenser. The working fluid is pumped back to the evaporator and the cycle is repeated. Organic fluids need to be adapted to current cycle conditions and equipment design. Some authors have investigated the effect of working fluids on the Rankine's organic heat recovery cycle. Basically, depending on the slope of the saturation vapor curve in the diagram (T-S), organic fluids can be classified into three categories. These include: dry, isentropic, and wet fluids, with the slope of the saturation vapor curve in positive, infinite and negative order, respectively. Many researchers have made significant efforts to optimize parameters with either thermodynamic performance (thermodynamic efficiency, net output power, exergy efficiency) or economic factors (net power to heat transfer ratio, heat exchanger level per unit of output power (APR), Energy price level (LEC), electricity cost (EPC). are assigned as a function target. In the meantime, few studies have focused on dual-objective optimization with respect to both thermodynamic efficiency and economic factors to Worth. Somayaji et al. [3] reported that dry and isentropic fluids perform better than the R113, R123, R245ca, and isobutene fluids because after expansion in the turbine, they do not distill. Conversely, more fluid distillation may Bear the risk of damaging the turbine. Hettiarachchi et al. [4]. considered the ratio of the overall heat exchanger level to the net output power (EPS) as a target function in order to find the optimal design for the ORC systems and concluded that R123 and pentane-n could be suitable fluids. The purpose of this study is to design an organic Rankine cycle with

simultaneous generation of electricity and heat and assuming the use of condenser output heat. As a result, the design has tried to keep the condenser outlet temperature as high as possible. Moreover, the method on the decrease, of the condensing temperature and growing the evaporating temperature by attraction heat pump to amend an ORC cycle proficiency was found in the research work of Chaiyat and Kiatsiriroat [5]. In this regard, Qiu et al., [6] experimentally tested a 50 (kW) bio-biodegradable organic cogeneration system based on the power and heat cogeneration system for domestic use. Heating was applied to the floor. Their results showed that the designed system produced 861 watt power with an efficiency of 1.41(%) and 47.26 (kWh) with efficiency of 78.69(%). Stalfi et al. [7] Studied the technical feasibility study of a centralized solar combined system and a dual geothermal power plant based on the organic fluid Rankine cycle. Using a parabolic solar farm as a source of high-cycle temperature, they estimated the cost of generating power depending on the location of the power plant at 215 (\$) per megawatt hour. Pribinger et al. [8] investigated thermodynamics by selecting the appropriate operating fluid and pressure level of a two-stage biomass burner organic fluid cycle for the simultaneous generation of heat and power with a focus on optimizing energy efficiency. Wang et al. [9], investigated various fluids to find the most appropriate working fluid for the cycle. Among the working fluids selected by them, R11, R141b, R113 and R123 are prominent due to their high dynamic thermal efficiency. While ignorance seems to be the R245fa and R245ca most important of the four fluids, while they seem to be biological. They found that heat source temperature, turbine inlet pressure, and fluid mass flow had a significant effect on thermal efficiency. Despite the different heat sources, it has become an interesting issue among the researchers. In the case of ORC systems, the heat dissipated from the micro-turbine is used as a heat source for the ORC cycle and generates additional surplus electricity. For high thermal demand plants, (MT-CHP) system efficiency can be higher than 80(%). On the other hand, the organic cycle of generating surplus electricity by using available heat has increased the

efficiency of pure electricity generation of a micro-turbine power plant by about 8-10%[10]. Micro turbines are sometimes used in medium to large installations to provide backup power in cases of power outages. However, simple micro turbines with a power generation efficiency of up to 30% are not a good economic proposition for the power grid, and many installations cannot justify installation and operating costs until they are provided with continuous electrical power. In many cases, by increasing the net fuel, the energy conversion efficiency of micro-turbines been offset. Gaseous and liquid fuels such as natural gas, liquefied petroleum gas (LPG), propane, landfill gas, digestive gas, diesel, biogas and kerosene are counted as micro-tube feedstock, Some of them are renewable sources[11]. ORC could be worked with down temperature heat source like low pressure saturated steam or hot water, but very little, study on the external irreversibility in the course of heat exchange with these heat sources at the ORC evaporator has been reported. Recently, fossil fuels and biomass have been used to raise the heat source. Biomass is a renewable source of energy derived from biomaterials and generally bio-waste. Furthermore, biomass fuels can be exploited to deliver governable energy and in the absence of other green energy such as wind solar to been used. Therefore, biomasses are the potential main, future renewable energy resources, with expanded bio-energy systems being considered as fundamental contributors to future sustainable energy manufacture [12, 13]. This fuel can vary depending on the location of use. For example, in areas where there is a corn farm, corn waste can be used as biomass fuel. Pyrolysis is an significant fundamental process that can be operate to study the thermochemical transmutation of biomasses into the biomass char and gaseous or liquid fuels [14]. It also improves gasification, stable carbon content, calorie value, and combustion processes. The combustion process is of great importance in boilers and kiln, that's why a sound science of this process is necessary to determine the possibility of the biomass fuels [15,16]. Therefore, considering environmental impacts on energy production, it is better to seek clean energy such as solar energy. Solar energy is one

of the biggest, most lasting and affordable types of energy source [17]. Solar collectors are appropriate devices, which are been exploited either produce electricity directly from sun or heating depending on the type of the collector. however, solar energy has many benefits, their intermittency is still worrying as when we want it such as night, it is not accessible. Using solar collectors is one solution to generate the energy that researchers have used from this clean energy in their own research. Calise F et al.[18] Conducted a technical evaluation of the organic Rankine cycle with a fluorescent solar pentane and solar energy source to generate power and heat at temperatures of 118(°C) to 230 (°C). They achieved an electrical efficiency of 9 to 10(%) and They concluded that such a plan would be economically feasible for most Mediterranean regions with a capital return period of about 10 years .It is now important for us to consider which of these energy sources is most economically viable for power generation, in the following section .In this study, while designing a proper organic Rankine cycle from a thermodynamic point of view, a detailed parametric study of the designed cycle and the effect of each of its effective parameters on performance has been investigated. The choice of organic fluid also affects the cycle efficiency. The effect of several different fluids on cycle efficiency is investigated. In a comprehensive review, the use of available energy sources, including solar energy, biomass as renewable energy (based on local conditions), fossil fuel, and micro turbine as non-renewable sources, has been examined. Thermodynamic and economic modeling has been performed for all components of the Rankine cycle, solar collector, micro turbine and biomass. Now by comparing different sources and fluids it finds the best source of energy and working fluid in terms of net power and energy efficiency, economic and environmental.

2. Problem description

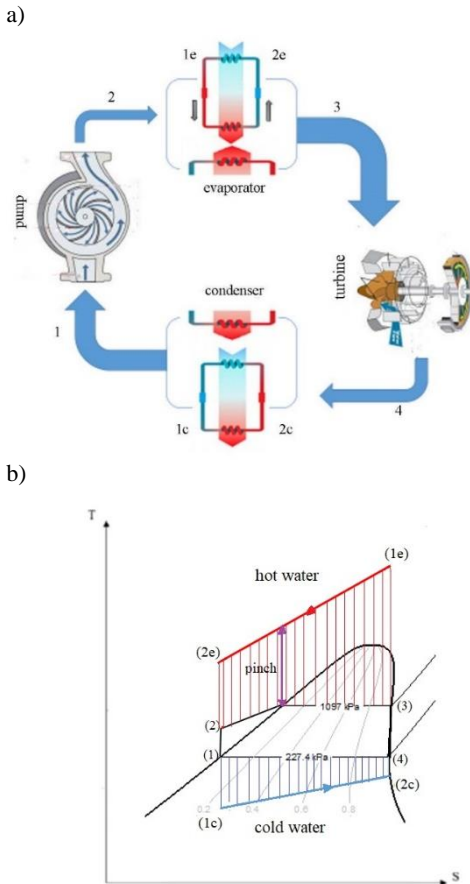


Figure 1.a) schematic of the Rankine cycle and b) diagram T-S of cycle

The system consists of four main components: boiler, condenser, turbine and pump. The system schematic sketch is shown in Fig1a. The ideal Rankine cycle does not involve any internal irreversibility's and consists of the following four processes (Figure 1b):

1-2 Isentropic compression in a pump: Water enters the pump at state 1 as saturated liquid and is compressed isentropically to the operating pressure of the boiler. The water temperature increases somewhat during this isentropic compression process due to a slight decrease in the specific volume of water.

2-3 Constant pressure heat addition in a boiler: Water enters the boiler as a compressed liquid at state 2 and leaves as a superheated vapor at state 3. The boiler is basically a large heat exchanger where the heat originating from combustion gases, nuclear reactors,

or other sources is transferred to the water essentially at constant pressure. The boiler, together with the section where the steam is superheated.

3-4 Isentropic expansion in a turbine: The superheated vapor at state 3 enters the turbine, where it expands isentropically and produces work by rotating the shaft connected to an electric generator.

4-1 Constant pressure heat rejection in a condenser: steam at state 4 enters the condenser. At this state, steam is usually a saturated liquid-vapor mixture with a high quality. Steam is condensed at constant pressure in the condenser, which is basically a large heat exchanger, by rejecting heat to a cooling medium such as a lake, a river, or the atmosphere. Steam leaves the condenser as saturated liquid and enters the pump, completing the cycle.

1e-2e Hot water from heat source with high constant temperature was entered 1e, to the evaporator. then gave its energy to cycle fluid. And whit Low temperature odder side of evaporator 2e exited.

1c-2c Cold water from environment whit low constant temperature was entered 1c to the condenser. then taken its energy of cycle fluid. and whit high temperature was odder side of condenser 2c exited.

2.1. Thermodynamic modelling

In this section, thermodynamic modeling of all components of the cycle is discussed. Assumptions are intended for thermodynamic analysis: a) The power plant is in steady state, b) Kinetic energy and potential energy are neglected, c) Pressure drop in the cycle is ignored. The following equations are written for the components of a Rankin cycle based on the first law of thermodynamics for a steady state steady flow-control volume.

$$\dot{Q}_{ev} = \dot{m}_{ht} (h_3 - h_2) \quad (1)$$

$$\dot{W}_{tur} = \dot{m}_f (h_3 - h_4) \quad (2)$$

$$\dot{Q}_{co} = \dot{m}_f (h_1 - h_4) \quad (3)$$

$$\dot{W}_{pump} = \dot{m}_f (h_2 - h_1) \quad (4)$$

The net output power of the cycle is expressed as an Equation:

$$\dot{W}_{net} = \dot{W}_{tur} - \dot{W}_{pump} \quad (5)$$

The cycle energy efficiency is as follows as:

$$\eta_{1st\ law} = \frac{\dot{W}_{net}}{\dot{Q}_{ev}} \quad (6)$$

For pump and turbine, Isotropic efficiency is defined as follows:

$$\eta_{is,P} = \frac{h_2 - h_{1s}}{h_2 - h_1} \quad (7)$$

$$\eta_{is,T} = \frac{h_3 - h_{4s}}{h_3 - h_4} \quad (8)$$

The physical exergy of each point of the cycle can also be calculated according to equation (9),

$$\psi = \dot{m} \left[(h - h_0) - T_0 (s - s_0) \right] \quad (9)$$

Exergy balance in the steady system is written as follows:

$$W_{rec} = \sum \psi_{in} - \sum \psi_{ex} + \sum \dot{Q}_j (1 - T_0 / T_j) \quad (10)$$

In equation (10), ψ_{in} and ψ_{ex} are related to the physical exergy of inlet and exit, respectively, and j is related to the thermal source. If the system is adiabatic or there is no external heat source, then $\sum \dot{Q}_j (1 - T_0 / T_j)$ is not considered.

Thus the maximum produced work for an adiabatic or without heat source steady systems can be obtained according to equation (11),

$$W_{rec} = \dot{m} \left[(h_{in} - h_{ex}) - T_0 (s_{in} - s_{ex}) \right] \quad (11)$$

The exergy efficiency of the Rankine cycle is defined as,

$$\eta_{II} = W_{net} / W_{rec} \quad (12)$$

The irreversibility value of the turbine is used in relation to (13).

$$i_{tur} = w_{rev} - w_{actual} \quad (13)$$

Where w_{actual} is an actual work of turbine.

The irreversibility value of the turbine is used in relation to (13).

$$i_{tur} = w_{rev} - w_{actual} \quad (13)$$

Where w_{actual} is an actual work of turbine.

2-1-1 Solar tower

Figure 2a shows a schematic of a solar tower with a hollow receiver Based on the modeling done by Lee [19, 20]. For thermal modeling of the solar tower, has been divide it into several sections and determine the losses in each section and finally calculated the

amount of heat absorbed by the fluid. In the present analysis, due to the complexity and dependence of the relationships, for a given absorbed energy and the unknown amount of mirror area, this model was not a closed solution. And so the solution algorithm is considered as shown in Figure 2b. The energy received by the central receiver is not fully absorbed and some of this energy is wasted as conductive, convection, emission and reflection heat loss.

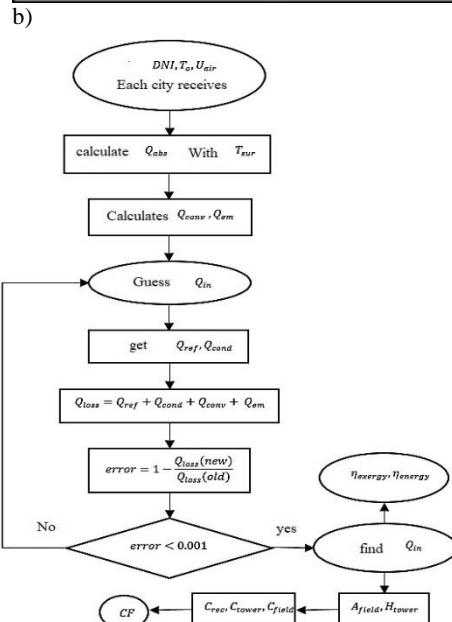
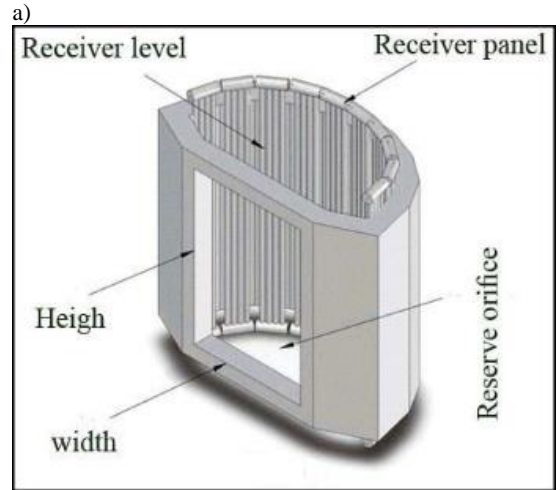


Figure2. a) schematic of solar tower and b) flow chart of solar tower computing algorithm

Therefore, the amount of heat absorbed by the fluid is written as a relation (14):

$$\dot{Q}_{abs} = \dot{Q}_{rec} - \dot{Q}_{heatloss} \tag{14}$$

where $\dot{Q}_{heatloss}$ is the amount of total heat dissipation and \dot{Q}_{abs} is the amount of heat absorbed by the fluid. The amount of total heat dissipation is obtained by the equation (15).

$$\dot{Q}_{heatloss} = \dot{Q}_{em} + \dot{Q}_{cond} + \dot{Q}_{conv} + \dot{Q}_{ref} \tag{15}$$

The convective heat loss consists of both forced and natural convection. The natural convective heat transfer coefficient of inside and outside of the receiver was given by equation (16) [20],

$$h_{air,nc,insi} = 0.81(T_{sur} - T_{air,nc,insi})^{0.426} \tag{16}$$

$$T_{air,nc,insi} = (T_{sur} + T_0) / 2$$

Where $h_{air,nc,insi}$ is equal to the convective heat transfer coefficient inside the receiver and is

$$h_{air,nc,o} = 1.24(T_{insu} - T_0)^{1/3} \tag{17}$$

where $h_{air,nc,o}$ is the convective heat transfer coefficient outside the receiver. The forced convective heat loss is considered from a flat plate and equal to the aperture. The heat transfer coefficient is defined as follow as:

$$Nu_{air,fc,insi} = 0.0287 Re_{air,insi}^{0.8} Pr_{air,insi}^{1/3} \tag{18}$$

Also, the Nusselt number outside the receiver can also be calculated by the equation (19).

$$Nu_{air,fc,o} = 0.0278 Re_{air,o}^{0.805} Pr_{air,o}^{0.45} \left(0.785 T_{insu,w} / T_0 \right)^{0.2} \tag{19}$$

As a result, the value of the overall convective heat transfer coefficient for air is calculated as follow as

$$h_{air,0} = \left(h_{nc,o}^a + h_{fc,o}^a \right)^{1/a} \tag{20}$$

Which is a = 1 for the cavity receiver. The amount of total convection heat loss can also be obtained as follows

$$\dot{Q}_{conv} = h_{air} (T_{sur} - T_0) A_{sur} \tag{21}$$

$$h_{air} = \left[h_{air,fc} + h_{air,nc} / F_r \right] \tag{22}$$

The conductive heat loss is estimated by equation (23).

$$\dot{Q}_{cond} = \frac{A_{sur} (T_{sur} - T_0)}{\left(\delta_{insu} / k_{insu} + 1 / h_{air,0} \right)} \tag{23}$$

Which T_{SUR} is calculated by means of equation(24)

$$\frac{\dot{Q}_{rec}}{A_{sur}} = \frac{(T_{sur} - \bar{T}_{ms})}{d_0 / d_i / \bar{h}_{ms} + d_0 Ln(d_0 / d_i) / 2 / k_{tube}} \tag{24}$$

$$\bar{T}_{ms} = \frac{T_{mi} + T_{mo}}{2}$$

Radiation heat loss is caused by the large difference in temperature between the receiving surface and the surrounding environment and is characterized as follows:

$$\dot{Q}_{em} = \epsilon \sigma (T_{sur}^4 - T_0^4) \tag{25}$$

Where σ represents Stephen Boltzmann's constant. The last type of heat loss is reflective loss. This loss is due to the reflection of the radiation from the receiving surface and depends on the type of material used in making it. Radiation heat dissipation is determined by the relation (26).

$$\dot{Q}_{ref} = \rho \dot{Q}_{rec} F_r \tag{26}$$

It is defined that the energy efficiency at the center of receiver as the ratio of absorbed energy to the input energy and the exergy efficiency as the absorbed exergy to the input exergy, which denotes equations (27) and (28).

$$\eta_{energy} = \dot{Q}_{abs} / \dot{Q}_{rec} \tag{27}$$

$$\eta_{exergy} = \dot{m}_{in} C_{pms} [(T_{mo} - T_{mi}) - T_0 Ln(T_{mo} / T_{mi})] / \dot{Q}_{rec} (1 - T_0 / T_s) \tag{28}$$

2-1-2- Micro turbine

Micro turbines are sometimes used in large installations as backup power supplies in the power plant. In the case of the organic Rankine cycle, the heat lost from the microturbine can be used as a heat source for the cycle. The heat production process is achieved in micro-turbines by giving a specific amount of work that can vary for each micro-turbine. The power of selected micro-turbine is about 100 to

200 (kW). The generated heat by micro turbine[10] can be calculated by equation (29)

$$\dot{Q}_{ex} = 1.337\dot{W}_{net,MT} + 28.69 \quad (29)$$

Where $\dot{W}_{net,MT}$ is the net power of micro turbine. The equation(29) is obtained for a power range of 8-950 (kW) with an error of 5(%) .

Moreover, the micro turbine can produce work except of the heat. that cycle efficiency with micro turbine it will be calculated with Equations (30) and (31).

$$\dot{W}_{total} = \dot{W}_{net} + \dot{W}_{MT} \quad (30)$$

$$\eta_{1^{st}law_{MT}} = \frac{\dot{W}_{total}}{\dot{m}_r LHV} \quad (31)$$

2-1-3- Biomass

In the application of biomass, waste products are produced on the basis of biomass in boilers and water vapor is produced. The total heat released from the biomass can be calculated from Equation (32)[21].

$$\dot{Q}_{gen} = \dot{m}_{bio} (h_{bio} - h_o) \quad (32)$$

Assuming total combustion efficiency of 15(%) and 65(%) efficiency for the biomass boiler, the heat transferred to the boiler is based on equation (33).

$$\dot{Q}_{boiler} = 0.8 \times 0.9 \dot{Q}_{gen} \quad (33)$$

2-2-Economic Modeling

The initial cost of the Rankin cycle includes the cost of the turbine, pump, condenser and boiler. In contrast to other costs, the cost of piping has been neglected. The initial cost of the Rankin cycle is approximated as follows:

$$C_{RC} = b_1 w_t^{d_1} + b_2 A_{cond}^{d_2} + b_3 A_{boiler}^{d_3} + b_4 w_p^{d_4} \quad (34)$$

The values b and d are specified by [22] . In this paper, the b values are [1673 4750 150 3500] and the d values are [0.8 0.47 0.8 0.75]. If a solar collector or micro turbine is used, the cost of new components will be added to the initial cost of the cycle. Modeling of other components is presented below.

2-2-1-Solar collector

The cost function for building a solar tower includes costs such as the cost of tower height, the cost of the equipment inside the receiver and consider the cost of mirrors needed to reflect light. The cost function for a solar tower is defined as an equation (35)[23].

$$CF = C_{tower} + C_{rec} + C_{heliostats} \quad (35)$$

The relationship between the cost of building the tower and the height of the tower can be defined as a relation (36)[24].

$$C_{tower} = 250,000 + 14.77(0.6806Q_{rec} + 106.6)^{2.395} \quad (36)$$

It should be noted that in the above relation Q_{rec} is in (MW). The cost of mirrors is estimated using Equation (37)[24].

$$C_{Heliostats} = 140A_n \quad [€] \quad (37)$$

The cost to the receiver is approximated using the equation (38)[25].

$$C_{rec} = \frac{46438}{\dot{q}_{rec}} + 21.899 \left[\frac{€}{Kw} \right] \quad (38)$$

Where \dot{q}_{rec} denotes the input flux to the receiver in (kW).

Taking into account the life of the equipment (n) and the annual profit(i) based on the report of the Central Bank, the investment cost is approximated. To obtain the cost of an investment in one year, the following is used to define the capital recovery factor (39).

$$CRF = \frac{i(1+i)^n}{(1+i)^n - 1} \quad (39)$$

In this study, the values of i and n are 0.137 and 25 years, respectively. Taking into account the cost of repairs equal to 0.02 the cost of the equipment is ultimately the cost of the collector is estimated as follows:

$$C = \frac{PEC}{CRF} + 0.02PEC \quad (40)$$

2-2-2- Waste heat recovery in micro turbine

The cost of the micro-turbine cycle is obtained from formula[10] (41).

$$C_{MT} = (b_1 \dot{W}_{MT} + d_1) + b_2 \dot{W}_{in}^{d_2} + b_3 A_{cond}^{d_3} + b_4 W_p^{d_4} \tag{41}$$

In this paper, the b values are [1673 4750 150 3500] and the d values are [0.8 0.47 0.8 0.75]. The cost of fuel required for a micro-turbine is obtained from equation (42).

$$C_f = 3600 \dot{m}_f \zeta \Psi_f \tag{42}$$

The environmental cost of carbon dioxide emissions is extracted from equation (43).

$$C_{inv} = \dot{m}_{totalCO_2} \dot{W}_{netMT} \zeta \Psi_{em} \tag{43}$$

Where Ψ_f, Ψ_{em}, ζ and $\dot{m}_{totalCO_2}$ are the fuel cost, the emission costs, System operating hour information per year and the amount of CO_2 [10].

2-2-3 Biomass

Biomass is a renewable source of energy derived from biomaterials. Generally, waste that is biologically derived from cell proliferation is called biomass. Table1 shows the price and energy production rate of some vegetable waste.

Table1. Energy and cost characteristics of biomass materials[24-26]

Biomaterials	Released Heat (kJ/kg)	Cost(\$/Ton)
Wheat waste	17000	30
Waste of tomatoes	16000	60
Potato waste	25000	20

2. Results & Discussion

Using the thermodynamic modelling performed for the Rankine power cycle with organic fluid, the first and second law of thermodynamics for different cycle states are investigated. The effects of pinch temperature, mass flow rate, cost of primary energy production with various sources, and environmental effects of the ORC were carefully studied. This section, first deals with the model validation presented for the solar tower and the Rankin cycle.

Table2. Input parameters of the solar tower[19]

d_i	0.019(m)	wind speed	5(m/s)
d_o	0.02065(m)	Pass number	12
k_{tube}	19.7(W/m.k)	δ_{ins}	0.07(m)
ϵ	0.8	Solar tower height	6(m)
τ	0.04	A_{sur}	21.2(m ²)

Table 3. Thermal analysis using the proposed model

$\eta_{energy}(\%)$	87.73
$Q_{conv}(kW)$	185.35
$Q_{em}(kW)$	296.7
$Q_{ref}(kW)$	207.66
$Q_{cond}(kW)$	10.04
$Q_{total}(kW)$	699.85

Table 4. The conditions for calculating the ideal ORC performance [27]

Parameters	Given values
Heat source temperatures at pinch point	80, 90, 100, and 110 (°C)
Pinch between heat source and evaporating temperatures	1–10 (°C)
Expander isentropic efficiency	0.85(%)
Working fluid isobutene	Tb=15.14 (°C) $\dot{m}_f= 1\text{kg/s}$
Cooling water	$T_{in}=30$ (°C), $\dot{m}_{cw} = 2(\text{kg/s})$
Expander inlet pressure	1097.1 (kPa)
Expander outlet pressure	227.4 (kPa)
Expander inlet temperature	93.7 (°C)
Expander outlet temperature	37.1(°C)
Isentropic efficiency of expander	71.4(%)

The solar tower is considered in accordance with the experimental data [19] shown in Table 2. Inlet and outlet temperatures to the solar tower are 50 (MW) at 290 (°C) and 595 (°C). The results of the proposed model are presented in Table 3. The efficiency of the solar tower considered in [19] is about 0.85-0.9 with an average thermal efficiency of 87(%) which is in full agreement with the result of the proposed model

87.77%) which indicates the accuracy of the proposed analytical model.

To ensure the validity of the modelling results presented in this study, Rankine cycle parameters are considered in accordance with Table 4. Table 5 shows a comparison between the results of the present study and the reference [27]. The percentage of deviation is about 7(%) -11(%), indicating a good agreement between the results of the present study and the reference [27]

Table5. Validation of Organic Rankine Cycle conditions different η_I in present study η_I Reference [27]

conditions	different	η_I in present study	η_I Reference [27]
Condition1	0.07	8.73(%)	9.40(%)
Condition2	0.072	8.17(%)	8.81(%)
Condition3	0.11	6.64(%)	7.73(%)

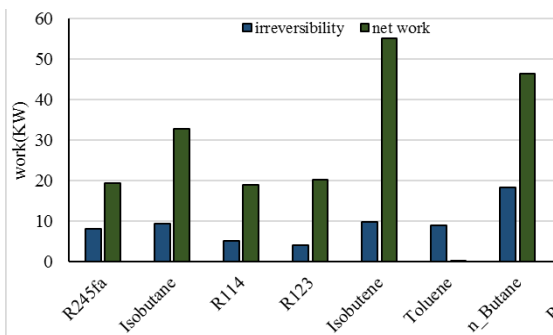


Figure3. The irreversibility and production work of the Rankine cycle with different fluids

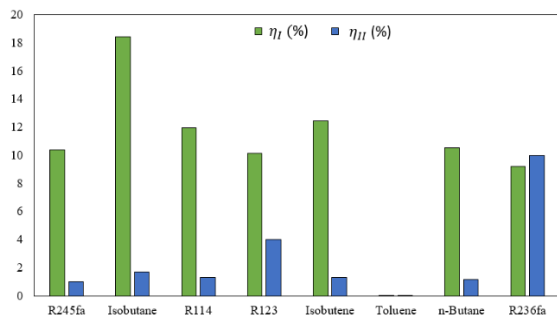


Figure 4. Rankine cycle performance with different fluids

The effect of different fluids on cycle performance is investigated. For this purpose, R245fa, Isobutane, R114, R123, Isobutene and Toluene are considered as

working fluid. Figure 3 shows the effect of different fluids on the net productive power of the cycle, irreversibility, the efficiency of the first and second law of thermodynamics. Results show that the highest and lowest production power belonged to isobutene and R114, respectively. The highest and the lowest irreversibility were for n-Butane and R123, respectively. Figure 4 shows the change in the efficiency of the first and second law with different ORC's working Fluid. The heat input to the cycle is the same for all fluids. It can be seen that most of the first law yields belong to isobutene. Therefore, isobutene has been selected as the operating fluid of the cycle for further investigation. Effect of T_{pinch} on the cycle efficiency is shown in Figure 5. The efficiency of the second law of the cycle decreases by increasing the pinch temperature from 85 (°C) to 110 (°C). One of the irreversible factors is heat transfer with temperature difference. Therefore, as the pinch temperature increases, the amount of irreversibility increases and the efficiency of the second law of the power cycle decreases.

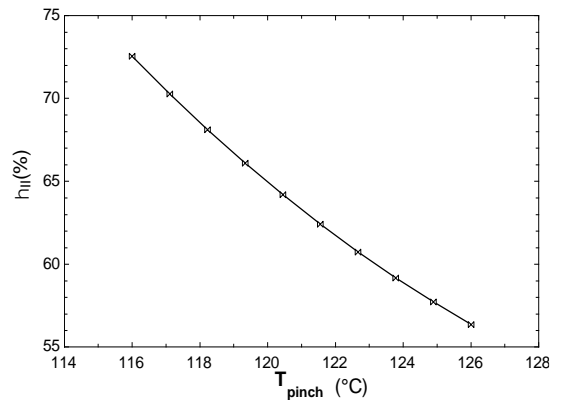


Figure 5 Effect of T_{pinch} on the ORC cycle

Figure 6 shows the influence of fluid flow inlet flow changes on second law cycle efficiency. Results show the second law efficiency is inversely related to the increase in the input flow rate. The reason is that with the amount of heat absorbed increases and the cycle cannot work longer than the (\dot{W}_{net}). Various sources have been considered to provide input heat to the cycle. The heat input to the cycle is assumed to be the same for all sources and is economically evaluated with respect to the modelling provided for each energy source.

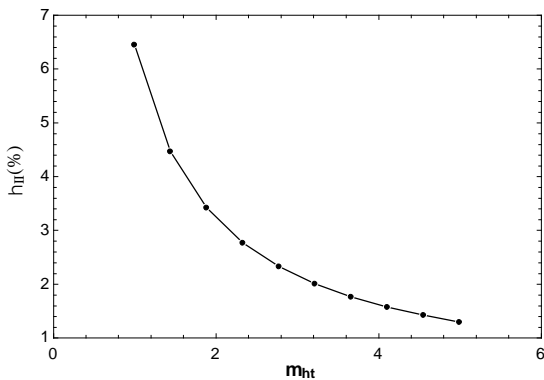


Figure 6. The effect of hot water flow rate on the ORC performance

The cost per kilowatt-cycle of production work for different energy sources is illustrated in Figure 7. The results show that the highest and lowest production costs are related to the MT-ORC and Hot water-ORC. In calculating the cost of a solar tower, more than 70(%) of the cost is related to the cost of mirrors. When using a micro turbine as an energy source, the net power of the cycle increases by about 20(%). The cost of biomass-generated power is approximately similar to that of hot water.

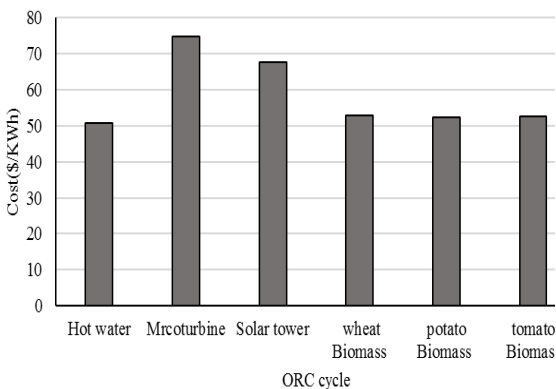


Figure 7 Price of power generated by different energy sources

4. Conclusions

This paper deals with the energy and economic modeling of the Rankin cycle combination with solar tower, micro turbine, hot water and biomass. The Rankine cycle efficiency was evaluated with several organic fluids and isobutene was selected as the working fluid. The results show that by increasing the

pinch temperature, the efficiency of the second law of the cycle decreases. Energy and economic modelling of the solar tower was performed. Considering the heat required by the power cycle, the solar tower was designed. The results show that over 70(%) of the solar tower cost is related to the cost of mirrors. The results show that the micro turbine-ORC system is costly while increasing the power output of the cycle by about 20(%). The solar tower-ORC system is in second place. The lowest cost is related to Hot water-ORC system. The biomass energy source system is economically competitive with the biomass system due to the biomass material.

Nomenclature

\dot{Q}	heat transfer rate (kW)
T	temperature ($^{\circ}\text{C}$)
v	specific volume (m^3/kg)
P	pressure (kPa)
p	pinch temperature difference ($^{\circ}\text{C}$)
h	specific enthalpy (kJ/kg)
s	specific entropy (kJ/kg K)
\dot{W}	Power (kW)
\dot{I}	exergy destruction rate (kW)
η	ORC component efficiency or cycle energy or exergy efficiency
k	Thermal conductivity (W / mK)
Q	Heat (W)
H_{tc}	Heat transfer coefficient
F_r	Shape coefficient
U	Speed (m / s)
CF	Cost function (Euro)
C	Cost
Nu	Nusselt number
Pr	Prandtl number
d	Diameter (m)
A	Area (m^2)
H	Height (m)
ρ	Coefficient of reflection
ϵ	emissivity coefficient
Ψ	Exergy
i	irreversible
Subscripts	
i	initial state
o	dead state or ambient
p	pump
tur	turbine
e	evaporator
f	working fluid

b	boiling point
c	condenser
cw	cooling water
η_I	law first law efficiency of the cycle
η_{II}	second law efficiency of the cycle
in	inlet
DNI	Vertical radiation per unit area
fc	Forced convection
nc	Natural convection
ins	Insulation
sur	Surface
out	Outside (around)
em	emission
ref	Reflection
abs	Absorb
conv	convection
cond	Conductivity
rec	receiver
mo	Output salt temperature
mi	Inlet salt temperature
ms	Molten salt
mir	mirrors
Sun	Sun
LHV	Thermal value of the lowest fuel
r	Fuel used in micro turbines
MT	Micro turbine

References

1. Kanbur, B.B., et al., *Cold utilization systems of LNG: A review*. Renewable and sustainable energy reviews, 2017. **79**: p. 1171-1188.
2. Borsukiewicz-Gozdur, A., *Dual-fluid-hybrid power plant co-powered by low-temperature geothermal water*. Geothermics, 2010. **39**(2): p. 170-176.
3. Somayaji, C., P. Mago, and L. Chamra. *Second law analysis and optimization of organic Rankine cycle*. in *ASME 2006 Power Conference*. 2006. American Society of Mechanical Engineers Digital Collection.
4. Hettiarachchi, H.M., et al., *Optimum design criteria for an organic Rankine cycle using low-temperature geothermal heat sources*. Energy, 2007. **32**(9): p. 1698-1706.
5. Chaiyat, N. and T. Kiatsiriroat, *Analysis of combined cooling heating and power generation from organic Rankine cycle and absorption system*. Energy, 2015. **91**: p. 363-370.
6. Qiu, G., et al., *Experimental investigation of a biomass-fired ORC-based micro-CHP for domestic applications*. Fuel, 2012. **96**: p. 374-382.
7. Astolfi, M., et al., *Technical and economical analysis of a solar-geothermal hybrid plant based on an Organic Rankine Cycle*. Geothermics, 2011. **40**(1): p. 58-68.
8. Preißinger, M., F. Heberle, and D. Brüggemann, *Thermodynamic analysis of double-stage biomass fired Organic Rankine Cycle for micro-cogeneration*. International Journal of Energy Research, 2012. **36**(8): p. 944-952.
9. Wang, E., et al., *Study of working fluid selection of organic Rankine cycle (ORC) for engine waste heat recovery*. Energy, 2011. **36**(5): p. 3406-3418.
10. Mago, P.J. and R. Luck, *Evaluation of the potential use of a combined micro-turbine organic Rankine cycle for different geographic locations*. Applied energy, 2013. **102**: p. 1324-1333.
11. Asgharian, P. and R. Noroozian, *Modeling and Efficient Control of Microturbine Generation System With Battery Energy Storage for Sensitive Loads*. Iranian Journal of Electrical and Electronic Engineering, 2019. **15**(1): p. 76-86.
12. McNamee, P., et al., *The combustion characteristics of high-heating-rate chars from untreated and torrefied biomass fuels*. Biomass and bioenergy, 2015. **82**: p. 63-72.
13. Hai, I.U., et al., *Assessment of biomass energy potential for SRC willow woodchips in a pilot scale bubbling fluidized bed gasifier*. Fuel, 2019. **258**: p. 116143.
14. Jayaraman, K. and I. Gökalp, *Pyrolysis, combustion and gasification characteristics of miscanthus and sewage sludge*. Energy Conversion and Management, 2015. **89**: p. 83-91.
15. Forbes, E., et al., *Physico-chemical characteristics of eight different biomass fuels and comparison of combustion and emission results in a small scale multi-fuel boiler*. Energy conversion and management, 2014. **87**: p. 1162-1169.
16. Hai, I.U., et al., *Experimental investigation of tar arresting techniques and their evaluation for product syngas cleaning from bubbling fluidized bed gasifier*. Journal of Cleaner Production, 2019. **240**: p. 118239.
17. Kizilkan, O., S. Khanmohammadi, and M. Saadat-Targhi, *Solar based CO2 power cycle employing thermoelectric generator and absorption*

refrigeration: Thermodynamic assessment and multi-objective optimization. Energy Conversion and Management, 2019. **200**: p. 112072.

18. Calise, F., et al., *Design and simulation of a prototype of a small-scale solar CHP system based on evacuated flat-plate solar collectors and Organic Rankine Cycle.* Energy Conversion and Management, 2015. **90**: p. 347-363.

19. Li, X., et al., *Thermal model and thermodynamic performance of molten salt cavity receiver.* Renewable energy, 2010. **35**(5): p. 981-988.

20. Benammar, S., A. Khellaf, and K. Mohammadi, *Contribution to the modeling and simulation of solar power tower plants using energy analysis.* Energy conversion and management, 2014. **78**: p. 923-930.

21. Mehmood, S., B.V. Reddy, and M.A. Rosen, *Energy analysis of a biomass co-firing based pulverized coal power generation system.* Sustainability, 2012. **4**(4): p. 462-490.

22. Darrow, K., et al., *Catalog of CHP technologies.* US Environmental Protection Agency, Washington, DC, 2015: p. 5-6.

23. Fritsch, A., C. Frantz, and R. Uhlig, *Techno-economic analysis of solar thermal power plants using liquid sodium as heat transfer fluid.* Solar Energy, 2019. **177**: p. 155-162.

24. Obidziński, S.a., *Pelletization of biomass waste with potato pulp content.* International Agrophysics, 2014. **28**(1).

25. Kolb, G.J., et al., *Power tower technology roadmap and cost reduction plan.* SAND2011-2419, Sandia National Laboratories, Albuquerque, NM, 2011. **7**.

26. Encinar J. M., G.J.F., Martinez G., *Energetic Use of Tomato Plant Waste.* International Journal of Fuel Processing Technology, 2008. **89**.

27. Kong, R., et al., *Thermodynamic performance analysis of a R245fa organic Rankine cycle (ORC) with different kinds of heat sources at evaporator.* Case Studies in Thermal Engineering, 2019. **13**: p. 100385.